The zinc transporter ZIP12 regulates the pulmonary vascular response to chronic hypoxia

The zinc transporter, ZIP12, regulates the pulmonary vascular response to chronic hypoxia

Lan Zhao[1†*], Eduardo Oliver[1*], Klio Maratou[4], Santosh S. Atanur[4], Olivier D. Dubois[1], Emanuele Cotroneo[1], Chien-Nien Chen[1], Lei Wang[1], Cristina Arce[1], Pauline L. Chabosseau[4], Joan Ponsa-Cobas[3], Maria G. Frid[7], Benjamin Moyon[5], Zoe Webster[5], Almaz Aldashev[6], Jorge Ferrer[3], Guy A. Rutter[2], Kurt R. Stenmark[7], Timothy J. Aitman[4, 8], Martin R. Wilkins[1]

[1] Centre for Pharmacology and Therapeutics, Division of Experimental Medicine, [2] Section of Cell Biology and Functional Genomics, Division of Diabetes, Endocrinology and Metabolism, and [3] Section of Epigenomics and Disease, Department of Medicine, Faculty of Medicine, Imperial College London, Hammersmith Hospital, London W12 0NN, United Kingdom. [4] Physiological Genomics and Medicine Group and [5] Transgenics and Embryonic Stem Cell Laboratory, Medical Research Council Clinical Sciences Centre, Hammersmith Hospital, London W12 0NN, United Kingdom. [6] Institute of Molecular Biology and Medicine, Bishkek, Kyrgyzstan. [7] Department of Pediatrics and Medicine, Division of Critical Care Medicine and Cardiovascular Pulmonary Research Laboratories, University of Colorado Denver, Denver, CO, United States. [8] Current address: Centre for Genomic and Experimental Medicine, University of Edinburgh, EH4 2XU, United Kingdom.[*] These authors contributed equally to this work.

[†]**Corresponding author:** Dr Lan Zhao. Centre for Pharmacology and Therapeutics, Experimental Medicine, Imperial College London, Hammersmith Hospital, Du Cane Road, London W12 0NN, UK. Telephone: 44-(0) 20 7594 6823; e-mail: l.zhao@imperial.ac.uk

The typical response of the adult mammalian pulmonary circulation to a low oxygen environment is vasoconstriction and structural remodelling of pulmonary arterioles, leading to chronic elevation of pulmonary artery pressure (pulmonary hypertension) and right ventricular hypertrophy. Some mammals, however, exhibit genetic resistance to hypoxia-induced pulmonary hypertension[1-3]. We used a congenic breeding program and comparative genomics to exploit this variation in the rat and identified the gene, *Slc39a12*, as a major regulator of hypoxia-induced pulmonary vascular remodelling. *Slc39a12* encodes the zinc transporter, ZIP12. We report that ZIP12 expression is increased in many cell types, including endothelial, smooth muscle and interstitial cells, in the remodelled pulmonary arterioles of rats, cows and humans susceptible to hypoxia-induced pulmonary hypertension. We show that ZIP12 expression in pulmonary vascular smooth muscle cells is hypoxia-dependent and that targeted inhibition of ZIP12 inhibits the rise in intracellular labile zinc in hypoxia-exposed pulmonary vascular smooth muscle cells and their proliferation in culture. We demonstrate that genetic disruption of ZIP12 expression attenuates the development of pulmonary hypertension in rats housed in a hypoxic atmosphere. This entirely novel and unexpected insight into the fundamental role of a zinc transporter in mammalian pulmonary vascular homeostasis suggests a new drug target for the pharmacological management of pulmonary hypertension.

We have reported previously that the Fisher 344 (F344) rat strain is resistant to hypoxia-induced pulmonary hypertension compared to the Wistar Kyoto (WKY) strain[2]. Linkage analysis of a F2 population derived from inbred WKY x F344 rats identified a quantitative trait locus (QTL) on chromosome 17[2]. Based on this observation, we next conducted ten successive microsatellite-guided backcrosses of offspring with WKY rats and derived two congenic strains in which the original QTL was dissected and represented as partially overlapping regions of a donor F344 genome interposed onto the genetic background of the WKY recipient strain (Extended Data Fig. 1, 2). Resistance to hypoxia-induced pulmonary hypertension was detected in one of the congenic strains (R47A, Fig. 1a-d, Extended Data Fig. 2). Three subcongenic strains (SubA, SubB and SubC) were derived by further backcrosses of R47A onto the WKY background and the congenic interval was fine-mapped to a region of 8.28 Mbp containing an estimated 65 genes (rat chr17: 85,072,475-93,347,784) (Fig. 1 and Extended Data Fig. 2a). Whole genome sequencing (>20X coverage) of the WKY and F344 parental strains[4] revealed 13 non-synonymous coding SNPs affecting 9 genes within the refined congenic interval, and 6 indels resulting in frameshift mutations in 4 genes (Extended Data Table 1). Polymorphic examination of the 13 SNPs and 6 indels in 2 additional rat strains susceptible to hypoxia-induced pulmonary hypertension (the spontaneously hypertensive and fawn-hooded rat strains, respectively) excluded 5 SNPs and 5 indels and narrowed the genes of interest to 7 (*Slc39a12, St8sia6, Cubn, Nmt2*, *Dclre1c*, *Hspa14* and *Cdnf,* Fig. 1e and Extended Data Table1). Further polyphen analysis allowed us to exclude 5 listed genes (*St8sia6, Cubn, Nmt2*, *Dclre1c* and *Cdnf)* as the non-synonymous coding changes were predicted to be benign. We identified *Slc39a12*, with a loss of thymidine at position 88,575,534 leading to a frameshift mutation in exon 11, as the highest priority candidate gene for further investigation.

Slc39a12 encodes the solute carrier 39 zinc transporter family (ZIP1 - 14) member 12 (ZIP12) and has high specificity for zinc[5]. The ZIP family tightly regulates cellular zinc homeostasis in numerous cell types by promoting zinc uptake from the extracellular space or release from intracellular compartments. The rat *Slc39a12* gene contains 12 exons and the ZIP12 protein comprises 688 amino acids with a secondary structure comprising 8 transmembrane domains (TMD). In the F344 strain the frameshift mutation in *Slc39a12* introduces a stop-codon predicting a C-terminal truncated ZIP12 protein of 553 amino acids (Extended Data Fig. 3a). This affects the conserved zinc transporting aqueous cavity between TMD IV to V, resulting in the loss of the metalloprotease motif (HEXPHE), which would be expected to lead to a reduction in zinc transport[6].

A pathognomonic histological signature of chronic hypoxia-induced pulmonary hypertension is thickening of the pulmonary vascular media (due to hyperplasia and hypertrophy of smooth muscle cells) and the muscularisation of previously unmuscularised pulmonary arterioles[7]. We found that ZIP12 mRNA levels were very low and ZIP12 protein undetectable by immunohistochemistry in the pulmonary vasculature of adult WKY rats housed in a normal oxygen atmosphere, but WKY rats exposed to hypoxia showed markedly increased lung ZIP12 mRNA levels and pronounced ZIP12 expression in remodelled pulmonary arterioles (Fig. 2a-b and Extended Data Fig. 3b). ZIP12 expression was evident in vascular smooth muscle but also other cell types (endothelial and interstitial cells) known to contribute to structural changes seen in hypoxic lungs. In contrast, and consistent with a frameshift mutation in *Slc39a12* predicting a C-terminal truncated protein, ZIP12 was undetectable with an antibody directed at the C-terminus of the protein in the lungs of chronically hypoxic F344 rats (Fig. 1b and Extended Data Fig. 3b).

Slc39a12 is highly conserved across species[8] and transcribed constitutively in many tissues (www/biogps.org). To investigate the relevance of our observations in rats to other

susceptible animal species, as well as humans, we examined ZIP12 expression in whole lung samples of 1) neonatal calves housed in a normal atmosphere or exposed to hypobaric hypoxia for two weeks (barometric pressure, PB = 445mmHg, equivalent to 4500m altitude, 12% O_2), 2) older (yearling) cattle with naturally occurring pulmonary hypertension (so-called "Brisket disease") developed as a result of prolonged pasturing at high altitude (2,438 to 3,505m), and 3) human subjects at sea level and Kyrgyz highlanders residing above 2500m. ZIP12 expression, which is undetectable by immunohistochemistry in healthy bovine and human lung exposed to a normal oxygen atmosphere (Fig. 2c), is clearly visible in the remodelled pulmonary vessels from chronic hypoxia exposure, indicating that ZIP12 up-regulation in pulmonary vasculature is a common response to hypoxia (Fig. 2c).

To better understand the regulation of ZIP12 by hypoxia, we exposed human pulmonary vascular smooth muscle cells in culture to hypoxia (2%O_2). Increased HIF protein and ZIP12 gene expression was observed in hypoxic cells; mRNA levels of other zinc transporters, ZIP6, ZIP7, ZIP10 and ZnT8, were unchanged (Extended Data Fig. 4a-b). Further examination of the *Slc39a12* gene using HOMER analysis[9] revealed a hypoxia response element (HRE) encoding both HIF-1α and HIF-2α binding motifs (Fig. 2d) at 1kb downstream of the ZIP12 transcription start site (human (hg19) chr10: 18,241,879-18,241,887). We cloned a 1.5kb fragment of the 5' region of ZIP12 containing this HRE into the luciferase reporter vector, pGL4.10 (Fig. 2d). Human pulmonary vascular smooth muscle cells transfected with the ZIP12 HRE reporter vector demonstrated significantly increased luciferase activity after exposure to hypoxia, while the luciferase activity of cells transfected with the mutant HRE vector (a substitution of the 5'-ACGTG-3' motif by 5'- AGCAG-3'; Fig. 2d) remained at basal normoxia levels (Fig. 2e). Chromatin immunoprecipitation (ChIP) followed by real time PCR confirmed the enrichment of both HIF-1α and HIF-2α binding to this ZIP12 HRE after hypoxia exposure (Fig. 2f).

We then explored the contribution of ZIP12 to the regulation of intracellular zinc levels in human pulmonary vascular smooth muscle cells. Intracellular labile zinc measured using a genetically-encoded fluorescence resonance energy transfer (FRET) based zinc probe, eCALWY-4[10], exhibited a striking increase in cells exposed to hypoxia for 48h, and this was markedly reduced by inhibiting ZIP12 expression with a targeted siRNA (Fig. 3a-e). Inhibition of ZIP12 expression with siRNA also inhibited hypoxia-induced pulmonary vascular smooth muscle cell proliferation (Fig. 3f). ZIP12 siRNA transfection did not affect intracellular zinc levels or proliferation in normoxia (Extended Data Fig. 4c-f). These data suggest that disrupted ZIP12 expression exerts a direct effect on pulmonary vascular cells in response to hypoxia and contributes to the resistant pulmonary hypertension phenotype exhibited in F344 strain.

To provide direct genetic confirmation that disrupted ZIP12 expression attenuates the pulmonary vascular response to hypoxia we employed zinc finger nuclease technology[11] to introduce mutations in *Slc39a12* in the hypoxia-susceptible WKY rat strain. A mutant line was generated containing a frame-shift resulting in a truncated ZIP12 protein with loss-of-function (Extended Data Fig. 5). Inter-cross of heterozygous animals generated homozygous (ZIP12-/-), heterozygous (ZIP12+/-) and wild-type rats that were then exposed to hypoxia ($10\%O_2$) for 2 weeks. ZIP12-/- rats demonstrated lower pulmonary artery pressures, right ventricular hypertrophy and vascular remodelling than wild-type rats (Fig. 4a-c; Extended Data Fig. 6a-d) with ZIP12+/- rats exhibiting an intermediate phenotype. Wild-type rats resembled WKY rats after exposure to hypoxia showing markedly increased lung ZIP12 expression in the remodelled pulmonary arterioles, in contrast to the absence of expression in ZIP12-/- rats (Fig. 4d-e). Comparison of the ZIP12-/- response to hypoxia with the WKY and F344 parental strains reveals that mutation of *Slc39a12* is responsible for about 50% of the resistance observed in the F344 strain, highlighting the importance of *Slc39a12* as a hypoxia-

susceptibility gene but also suggesting that other genes yet to be identified may also contribute.

Systemic blood pressure and cardiac output in the hypoxic ZIP12-/- rats was similar to that of wild-type rats (Extended Data Fig. 6e-g) signifying that the reduced pulmonary artery pressures in the ZIP12-/- rat in chronic hypoxia is due to reduced pulmonary vascular resistance (PVR; mean pulmonary artery pressure = PVR x cardiac output). Both vascular tone and structural remodeling contribute to PVR, and increased pulmonary vascular tone preceeds the structural changes. ZIP12 expression may increase PVR by increasing pulmonary vascular tone. Zinc-thiolate signaling has been reported to mediate the constriction of pulmonary microvascular endothelial cells in acute hypoxia through activation of protein kinase C and inhibition of myosin light chain phosphatase, inducing stress fibre formation and endothelial cell contraction[12]. We have shown that ZIP12 targeted siRNA attenuates stress fibre formation in human pulmonary vascular smooth muscle cells cultured in hypoxia (Extended Data Fig. 6h-f). But given the time-dependent induction of ZIP12 expression in pulmonary vasculature by hypoxia, the main contribution of ZIP12 is likely to be in regulating the response to chronic rather than acute hypoxia. In further support of a direct effect on structural remodelling of pulmonary arterioles, we investigated angiogenesis *ex vivo* using pulmonary arteriole rings dissected from ZIP12-/- and wild-type rats. Vascular outgrowth from ZIP12-/- vessels in response to hypoxia was attenuated compared to vessels from wild-type rats (Extended Data Fig. 6j-k).

The underlying mechanisms through which ZIP12 affects hypoxic responses remain to be defined. Excess intracellular zinc concentrations mediated by upregulation of ZIP family members have been observed in a variety of tumour tissues and linked to cell proliferation and survival[13-15]. Zinc is a structural component of a large variety of intracellular proteins, including enzymes and transcription factors. Zinc binding motifs have been

identified in drug targets for pulmonary hypertension, for example, phosphodiesterase type 5 (PDE5) and histone deacetylases[16,17]. Reduced ZIP12 expression and intracellular labile zinc levels would be expected to inhibit PDE5 activity[18], and we have previously shown that PDE5 inhibition attenuated pulmonary vascular smooth muscle proliferation in culture[19].

Following on from our demonstration that ZIP12 is hypoxia-inducible and a key regulator of the pulmonary vascular response to chronic alveolar hypoxia exposure, we examined lung ZIP12 expression in other presentations of pulmonary hypertension where tissue hypoxia is an important driver of pathology. Again, in contrast to healthy lungs, ZIP12 expression was clearly evident in lung tissues from chronic iron deficient rats[20] and rats exposed to monocrotaline, as well as patients with idiopathic pulmonary arterial hypertension (IPAH) [21] (Fig. 4f), prominent in the remodeled pulmonary vasculature as identified by co-staining with smooth muscle actin (Fig. 4g). HIF-activation in these tissues was confirmed by upregulation of carbonic anhydrase IX, a recognized HIF-regulated biochemical signature of tissue hypoxia[22] (Extended Data Fig. 7). Interestingly, the F344 rat strain has previously been reported to exhibit some resistance to monocrotaline-induced pulmonary hypertension [23]; this was recapitulated in the ZIP12-/- rat (Extended Data Fig. 8). These data signal a fundamental role for ZIP12 in the regulation of pulmonary vascular homeostasis in hypoxic stress, relevant to the pathogenesis of pulmonary hypertension beyond that associated with life in a low oxygen atmosphere. The current treatments for pulmonary hypertension centre on the pharmacological manipulation of signaling mechanisms used by vasoactive factors and have limited therapeutic benefit. Our observations open a new avenue of research into the therapeutic potential of ZIP12 inhibition and suppressed excursions of intracellular free zinc as a novel strategy for preventing or treating pulmonary hypertension.

Online Content: Methods, along with any additional Extended Data display items and Source Data, are available in the online version of the paper; references unique to these sections appear only in the online paper.

Acknowledgements

This research was supported by successive grants from British Heart Foundation to M.R.W and L.Z. (PG/95170, PG/98018, PG/2000137, PG/04/035/16912, PG/12/61/29818, PG/10/59/28478 and RG/10/16/28575). G.A.R. was supported by a Wellcome Trust Senior Investigator Award (WT098424AIA), MRC Programme Grant (MR/J0003042/1) and a Royal Society Research Merit Award. We would like to thank Ana I. Garcia-Diaz from the Physiological Genomics and Medicine Group of the Medical Research Council Clinical Sciences Centre (MRC-CSC) for her kind advice on genotyping techniques; and Dr Rob Edwards from Experimental Medicine, Imperial College London for his advice on antibody production. We thank Professor Chris Haley from the Roslin Institute for helpful discussions on the rat genetic map.

Contributions

L.Z. and M.R.W. were principal investigators on grants from the British Heart Foundation, developed concepts and supervised the project. L.Z., M.R.W., and E.O. designed and implemented the experiments. T.A. gave conceptual advice on the congenic program and whole genome sequencing. L.Z., M.R.W., T.A., K.M., E.O. and O.D.D. conducted the congenic breeding program. S.S.A. analysed whole genome sequence data and performed the Polyphen analysis. L.Z., E.O. and O.D.D., with the support of B.M. and Z.W., generated the

ZIP12 transgenic rat. L.Z., E.C. and L.W. performed immunohistochemistry and immunofluorescence. E.O. conducted the in vitro cell culture experiment. C.A. and E.O. performed the angiogenesis assay. G.R. supervised and E.O. and P.L.C. conducted the intracellular labile zinc measurement experiments. C-N.C. and E.O. performed ChIP-PCR. J.P-C. and E.O. cloned the HRE construct and performed luciferase reporter assays. M.G.F., K.R.S. and A.A provided cattle and human lung sections. E.O. performed statistic analysis. L.Z., M.R.W., and E.O. interpreted the data and wrote the manuscript. T.A., G.R., J.F., S.S.A. and K.D. edited the manuscript.

Competing financial interests

The authors declare no competing financial interests.

Figure Legends

Figure 1. The pulmonary vascular response to hypoxia in the F344 rat is influenced by a region of chromosome 17 containing *Slc39a12*. a. A genetic map of 3 sub-congenic strains (SubA, SubB and SubC) derived from the R47A congenic strain (originally derived from a WKYxF344 cross) backcrossed with the WKY parental strain. The refined congenic region (orange) of 8.28Mb containing 65 genes is within the SubB strain. **b-d.** SubB exhibits attenuated pulmonary hypertension after 2 weeks exposure to a 10% O_2 atmosphere compared to WKY, SubA and SubC rats: **b.** mean pulmonary artery pressure (mPAP); **c.** right ventricular hypertrophy (RV/LV+Septum ratio) (n=17 WKY, 15 F344, 14 R47A, 8 SubA, 10 SubB, 10 SubC); **d.** vascular muscularisation (n=6 each group). Dotted line indicates mean measurements from all the rats in a normal oxygen atmosphere (21%O_2; mPAP = 14.7±0.3 mmHg; RVH=0.270±0.004; % muscularization=34.2±0.36; for actual values in rat strains see Extended Data Fig. 3). Values are expressed as mean ± standard error of the mean (SEM). *P<0.05, **P<0.01, ***P<0.001 compared to WKY after one-way

ANOVA analysis followed by Bonferroni correction for multiple testing. **e.** The genes of interest (*Slc39a12, St8sia6, Cubn, Nmt2*, *Dclre1c*, *Hspa14* and *Cdnf*) identified within the SubB congenic interval. The frameshift mutation in *Slc39a12* introduces a stop-codon, resulting in a truncated protein**.**

Figure 2. *Slc39a12* encodes a zinc transporter, ZIP12, which is up-regulated in pulmonary vascular tissue from mammals exposed to chronic hypoxia. a. ZIP12 mRNA levels in control and hypoxic WKY rat lungs (n=6 each group). **b.** Prominent ZIP12 immunostaining in remodelled pulmonary arterioles in WKY but not F344 rat lungs exposed to hypoxia. **c.** No ZIP12 staining was detected in pulmonary arteries of low altitude (normoxia control, CO calf) calves and sea-level humans, yet prominent ZIP12 immunostaining was observed in the remodelled pulmonary arteries of calves with severe pulmonary hypertension (Hx calf), in cattle naturally susceptible to pulmonary hypertension at altitude ("Brisket disease", BD), as well as Kyrgyz highlanders residing above 2500m. **d.** Design of the luciferase reporter vector pGL4.10 containing a 5' region of ZIP12 which includes a hypoxia response element (HRE) encoding for both HIF-1α and HIF-2α binding motifs or a mutant HRE sequence where the 5'-ACGTG-3' motif has been replaced by 5'-AGCAG-3'(mHRE). **e.** Human pulmonary artery smooth muscle cells (HPASMCs) transfected with the ZIP12 HRE reporter vector demonstrated a significantly increased luciferase activity after exposure to hypoxia, but not in the cells transfected with the mutant HRE vector (n=6 per group). **f.** Increased levels of HIF-1α and HIF-2α bound to the ZIP12 HRE assayed by ChIP-qPCR of chromatin from HPASMCs cultured in normoxia and hypoxic conditions (n=3 per group). Data are calculated as percentage of input levels, with the dotted line marking percentages below mock immunoprecipitation (IP). Values are expressed as mean ± SEM. *P<0.05, **P<0.01, ***P<0.001 compared to normoxic control

after One-Way ANOVA analysis followed by Bonferroni correction for multiple testing. NS, not significant.

Figure 3. ZIP12 knockdown inhibits hypoxia-induced increase in intracellular labile zinc concentration and proliferation of human pulmonary artery smooth muscle cells (HPASMCs). a. Representative wide-field microscope images of HPASMC transfected with eCALWY-4 probe. Hypoxia exposure produced a striking increase in intracellular free zinc (resulting in decreased FRET)[10]. This was inhibited by transfection with ZIP12 siRNA. TPEN-mediated Zn^{2+} chelation was used to derive maximum fluorescence and 100 μM $ZnCl_2$ in the presence of the Zn^{2+} ionophore and pyrithione (ZnPyr) was used to derive the minimum fluorescence. **b.** Representative traces showing the changes in fluorescence ratio of the eCALWY-4 probe. Steady-state fluorescence intensity ratio citrine/cerulean (R) was measured, then maximum and minimum ratios were determined to calculate free Zn2+ concentration using the formula: [Zn2+] = Kd×(Rmax-R)/(R-Rmin), where the Kd for eCALWY-4 is 630 pM, the maximum ratio (Rmax) was obtained upon intracellular zinc chelation with 50 μM TPEN and the minimum ratio (Rmin) was obtain upon zinc saturation with 100 μM ZnCl2 in the presence of the Zn2+ ionophore, pyrithione (5 μM)[10]. **c.** Quantification of intracellular zinc levels (n=10 each group). **d.** Chronic hypoxia (48h) increases ZIP12 mRNA levels in HPASMCs, which is inhibited by *Slc39a12* siRNA (n=5 each group). **e.** Representative immunoblot of ZIP12 demonstrating inhibition of hypoxia-stimulated ZIP12 protein expression by *Slc39a12* siRNA in HPASMCs (n=3). **f.** ZIP12 siRNA inhibits hypoxia-induced proliferation in HPASMCs (n=5 each group). *P<0.05, ***P<0.001 compared to control group, #P<0.05 compared to hypoxia group. Scr, scramble siRNA control.

Figure 4. Genetic disruption of ZIP12 in WKY rat attenuates hypoxia-induced pulmonary hypertension. a-c. Zinc finger nucleases were used to disrupt ZIP12 in the WKY strain. Rats deficient in ZIP12 demonstrate allele dose-dependent attenuation of hypoxia-induced pulmonary hypertension compared to wild-type (WT) rats: **a.** mean pulmonary artery pressure (mPAP); **b.** right ventricular hypertrophy (RV/LV+Septum) (normoxia groups: n=10 WT, 8 ZIP12+/-, 12 ZIP12-/-; hypoxia groups: n=14 WT, 16 ZIP12+/-, 12 ZIP12-/-); **c.** pulmonary arteriole muscularisation (n=5 each group). ***$p<0.001$ compared to normoxia WT group, #$p<0.05$ compared to hypoxia WT group after one-way ANOVA analysis followed by Bonferroni correction for multiple testing. **d.** ZIP12 was undetectable by Western blot in hypoxic ZIP12-/- rats but increased in hypoxic wide-type (WKY) rats (n=3 each group). **e.** ZIP12 expression by immunohistochemistry of WT and ZIP12-/- rat lungs before and after hypoxia (2 weeks). **f.** ZIP12 expression in lungs from a chronic iron deficient rat, monocrotaline (MCT) rat and a patient with idiopathic pulmonary arterial hypertension (IPAH). **g.** Double immunofluorescence demonstrates co-localisation of ZIP12 and smooth muscle actin in the remodelled vessels from the IPAH patient.

References

1 Wilkins, M. R. *et al.*. Pathophysiology and treatment of high-altitude pulmonary vascular disease. *Circulation* **131**, 582-590, doi:10.1161/CIRCULATIONAHA. 114.006977 (2015).

2 Zhao, L. *et al.* Right ventricular hypertrophy secondary to pulmonary hypertension is linked to rat chromosome 17: evaluation of cardiac ryanodine Ryr2 receptor as a candidate. *Circulation* **103**, 442-447 (2001).

3 Rhodes, J. Comparative physiology of hypoxic pulmonary hypertension: historical clues from brisket disease. *Journal of applied physiology* **98**, 1092-1100, doi:10.1152/japplphysiol.01017.2004 (2005).

4 Atanur, S. S. *et al.* Genome sequencing reveals loci under artificial selection that underlie disease phenotypes in the laboratory rat. *Cell* **154**, 691-703, doi:10.1016/j.cell.2013.06.040 (2013).

5 Chowanadisai, *et al.* Neurulation and neurite extension require the zinc transporter ZIP12 (slc39a12). *Proceedings of the National Academy of Sciences of the United States of America* **110**, 9903-9908, doi:10.1073/pnas.1222142110 (2013).

6 Liuzzi, J. P. & Cousins, R. J. Mammalian zinc transporters. *Annual review of nutrition* **24**, 151-172, doi:10.1146/annurev.nutr.24.012003.132402 (2004).

7 Schermuly, R. T., *et al.* Mechanisms of disease: pulmonary arterial hypertension. *Nature reviews. Cardiology* **8**, 443-455, doi:10.1038/nrcardio.2011.87 (2011).

8 Chowanadisai, W. Comparative genomic analysis of slc39a12/ZIP12: insight into a zinc transporter required for vertebrate nervous system development. *PloS one* **9**, e111535, doi:10.1371/journal.pone.0111535 (2014).

9 Heinz, S. *et al.* Simple combinations of lineage-determining transcription factors prime cis-regulatory elements required for macrophage and B cell identities. *Molecular cell* **38**, 576-589, doi:10.1016/j.molcel.2010.05.004 (2010).

10 Vinkenborg, J. L. *et al.* Genetically encoded FRET sensors to monitor intracellular Zn2+ homeostasis. *Nature methods* **6**, 737-740, doi:10.1038/nmeth.1368 (2009).

11 Cui, X. *et al.* Targeted integration in rat and mouse embryos with zinc-finger nucleases. *Nature biotechnology* **29**, 64-67, doi:10.1038/nbt.1731 (2011).

12 Bernal, P. J. *et al.* A role for zinc in regulating hypoxia-induced contractile events in pulmonary endothelium. *Am J Physiol Lung Cell Mol Physiol* **300**, L874-886, doi:10.1152/ajplung.00328.2010 (2011).

13 Zhang, Y. *et al.* ZIP4 regulates pancreatic cancer cell growth by activating IL-6/STAT3 pathway through zinc finger transcription factor CREB. *Clinical cancer research : an official journal of the American Association for Cancer Research* **16**, 1423-1430, doi:10.1158/1078-0432.CCR-09-2405 (2010).

14 Grattan, B. J. & Freake, H. C. Zinc and cancer: implications for LIV-1 in breast cancer. *Nutrients* **4**, 648-675, doi:10.3390/nu4070648 (2012).

15 Chen, Q. G. *et al.* The role of zinc transporter ZIP4 in prostate carcinoma. *Urologic oncology* **30**, 906-911, doi:10.1016/j.urolonc.2010.11.010 (2012).

16 Zhao, L. *et al.* Sildenafil inhibits hypoxia-induced pulmonary hypertension. *Circulation* **104**, 424-428 (2001).

17 Zhao, L. *et al.* Histone deacetylation inhibition in pulmonary hypertension: therapeutic potential of valproic acid and suberoylanilide hydroxamic acid. *Circulation* **126**, 455-467, doi:10.1161/CIRCULATIONAHA.112.103176 (2012).

18 Francis, S. H., *et al.* Zinc interactions and conserved motifs of the cGMP-binding cGMP-specific phosphodiesterase suggest that it is a zinc hydrolase. *The Journal of biological chemistry* **269**, 22477-22480 (1994).

19 Wharton, J. *et al.* Antiproliferative effects of phosphodiesterase type 5 inhibition in human pulmonary artery cells. *American journal of respiratory and critical care medicine* **172**, 105-113, doi:10.1164/rccm.200411-1587OC (2005).

20 Cotroneo, E. *et al.* Iron Homeostasis and Pulmonary Hypertension: Iron Deficiency Leads to Pulmonary Vascular Remodeling in the Rat. *Circulation research*, doi:10.1161/CIRCRESAHA.116.305265 (2015).

21 Tuder, R. M. *et al.* Expression of angiogenesis-related molecules in plexiform lesions in severe pulmonary hypertension: evidence for a process of disordered angiogenesis. *The Journal of pathology* **195**, 367-374, doi:10.1002/path.953 (2001).

22 Beasley, N. J. *et al.* Carbonic anhydrase IX, an endogenous hypoxia marker, expression in head and neck squamous cell carcinoma and its relationship to hypoxia, necrosis, and microvessel density. *Cancer research* **61**, 5262-5267 (2001).

23 Pan, L. C., *et al.* Strain Differences in the Response of Fischer-344 and Sprague-Dawley Rats to Monocrotaline Induced Pulmonary Vascular-Disease. *Toxicology* **79**, 21-35, doi:Doi 10.1016/0300-483x(93)90203-5 (1993).

Methods

Animals

Inbred Wistar-Kyoto (WKY, Charles River, UK) and Fischer 344 rats (F344, Harlan, UK) were used as original strains. Animals were maintained at a constant temperature (20°C to 22°C) with a 12-hour on/12-hour off light cycle, with food and water *ad libitum*. All experiments were conducted under the project licence PPL70/7425 in accordance with the UK Home Office Animals (Scientific Procedures) Act 1986 (London, UK). To ascertain the pulmonary artery pressure phenotype, male rats (WKY, F344, congenic and sub-congenic strains, ZIP12 transgenic rats) aged 10-12 weeks were studied in batches, with the parental WKY strain included as an internal control in each batch studied. Sample sizes were chosen on the basis of experience of pulmonary artery pressure variation in the parental strains. A sample size of at least n=5 per group was predicted to detect a difference in mean pulmonary arterial pressure ≥ 5mmHg (standard deviation = 3) with 95% power with 95% confidence. Additional animals were studied to obtain sufficient tissue for supportive analyses.

Generation of congenic and sub-congenic strains

To investigate the involvement of the chromosome 17 QTL in the pulmonary hypertension (PH) phenotype, we introgressed the F344 chromosome QTL segment into the WKY genetic background by repeated backcrossing[2]. We produced a congenic rat strain, R47A (WKY.F344-*D17Got91/D17Rat51*), which contains 15Mbp from the F344 donor region that maps to the distal end of the QTL on the WKY background.

Subsequently, we generated 3 sub-congenic strains Sub-A (WKY.F344-*D17Got91 /D17Rat47*), Sub-B (WKY.F344-*D17Rat47/D17Rat51*) and Sub-C (WKY.F344-*D17Rat131 /D17Rat51*). These three recombination events divide the R47A congenic interval into three smaller and overlapping sub-congenic intervals (Extended Data Fig. 1).

Microsatellite genotyping of congenic rats

Congenic and sub-congenic rats were genotyped using simple sequence length polymorphism (SSLP) markers (Extended Data Table 2). In order to reduce the unknown regions between the markers, rats were also genotyped using primers specifically designed to amplify known regions containing insertions or deletions in one of the two parental strains (Extended Data Table 2). Genomic DNA was isolated from rat ear clippings using Hot Sodium Hydroxide and Tris (HotSHOT) extraction[24]. Forward primers were fluorescently labelled with 6-FAM. PCR products together with the fluorescent size marker (ROX 400HD, Applied Biosystems) were diluted in formamide and run on a 3730xl DNA Analyzer (Applied Biosystems). Results were analysed using GeneMapper v3.7 software (Applied Biosystems).

Illumina Genome Sequencing Library preparations

Five micrograms of male WKY/Ncrl (two animals) and F344/Ncrl (one animal) rats were used to construct paired-end whole-genome libraries with 300-550 bp insert size. Genomic DNA was prepared by standard phenol chloroform extraction followed by treatment with DNAse free RNAse. DNA quality was assessed by spectrophotometry (260/280 and 260/230) and gel electrophoresis before library construction. Genomic DNA was sheared for 90 sec (Covaris S2, KBioscience, Herts, UK), using 10% duty cycle, 5 intensity and 200 cycles per burst. The shearing efficiency was assessed by Qubit 2.0 fluorometer measurements (Life Technologies Ltd, Paisley, UK) and gel electrophoresis. The library was prepared as recommended (Illumina Genomic DNA sample prep kit protocol) with 9 cycles of PCR amplification (Illumina Inc., Hayward, CA). Constructed libraries were assessed with an Agilent 2100 bioanalyser using a HS DNA assay (Agilent Technologies, Edinburgh, UK) and quantified using a KAPA Illumina SYBR Universal Lib QPCR kit (Anachem Ltd, Bedfordshire, UK). The resulting libraries were sequenced on an Illumina HiSeq2000

following the manufacturer's instructions. Polymorphisms were confirmed by capillary sequencing.

Generation and genotyping of WKY.*Slc39a12* (+/-) and (-/-) rats

CompoZr™ Custom Zinc Finger Nucleases targeting the rat *Slc39a12* gene were designed and purchased from Sigma-Aldrich (Extended Data Fig. 3). Pronuclei from fertilized WKY oocytes were microinjected with ZFN mRNA (2 ng/µl). Three out of eleven pups were positive for *Slc39a12* mutations, as revealed by Cel-I surveyor assay and gene sequencing[11]. One pup (mutant 77) hosted a stop codon 15 amino acids from the ZFN binding site, resulting in a truncated protein of 490 amino acids (54 KDa), 198 amino acids smaller than the wild type protein, and introduced a sequence coding for 5'-ATTTAAAT-3', a binding site for the SwaI restriction enzyme. Mutant 77 was selected as a founder to mate with a WKY female. Pups were genotyped by amplifying DNA and digesting with SwaI. The primers used to amplify the region of interest were forward 5'-GCAATGGTTTTCCACAGTGA-3' and reverse 5'-GCGCACTGAGGCTTTAAGAA-3'.

Pulmonary hypertension phenotyping

Pulmonary hypertension was induced by placing animals in a normobaric hypoxic chamber (FIO_2 = 10%) for 2 weeks or by subcutaneous injection of monocrotaline (60 mg/kg; Sigma-Aldrich). The experiments were not randomised. All studies were performed using the same equipment and all haemodynamic measurements made by the same two operators. The operators were blinded to the genetic status of animals, which was confirmed after phenotyping. All histological assessments were made by two observers blinded to genetic status of animals. At the end of each experimental period, animals were weighed and anesthetized (Hypnorm 1ml/kg *i.m.*; Mydazolam 0.8ml/kg *i.p.*). Pulmonary arterial pressure was measured with a pre-curved catheter inserted through the right jugular vein. Systemic

blood pressure was assessed via carotid artery cannulation. Cardiac output was measured by thermodilution. Pulmonary vascular resistance (PVR) was calculated using the standard equation: PVR = mean pulmonary artery pressure / cardiac output. All data were recorded with a PowerLab Data Acquisition system (AD Instruments) and analysed using LabChart 7 software.

The animals were then killed and the heart dissected and individual chamber weights recorded. The ratio of right ventricle to left ventricle plus the septum mass (RV/LV+sep) was calculated as RV hypertrophy index. Some collected tissues were snap frozen in liquid nitrogen and stored at -80°C for further biochemical measurements. The left lung was fixed by inflation with 10% formalin in phosphate-buffered saline, embedded in paraffin, sectioned for histology. Transverse rat lung sections were processed for elastic van Gieson (EVG) staining. Peripheral vessels <100 μm diameter were counted at x40 magnification objective and pulmonary vascular remodelling was expressed as the proportion of vessels with double elastic lamina (>75% of the circumference as fully muscularised, 25-75% as partially muscularised) to total vessels counted. Counting was performed twice by observers blinded to treatment.

Ex vivo angiogenesis assay of pulmonary arteriole

Angiogenesis assay of arterial rings was performed as previously described[25]. Pulmonary arterioles (1st and 2nd order) were dissected from rat lungs viewed under the microscope. One mm sections were placed in matrigel (50μl/well) in a 96-well plate, allowed to gel for 30mins at room temperature, then incubated for up to 6 days with endothelial cell culture medium MV2 with 5% foetal calf serum (PromoCell). On days 3, 4, 5 and 6, the length of the longest sprouts was measured under the microscope (4 x objective). On day 6 arteriole ring

fluorescent images were taken by staining the tissue with calcein (Invitrogen) for 15 minutes at 37°C.

Anti-ZIP12 Antibody production

An antibody raised against the five last amino-acids at the C terminus (Ct) of both the human and the rat ZIP12 protein was produced in rabbits following previous methodology[26]. Rabbits were immunized with synthetic peptides conjugated to keyhole limpet hemocyanin ([CYS(KLH)]QNIKI). Peptide sequence was confirmed to be ZIP12 specific using RStudio. Immunized rabbit serum containing anti-ZIP12 antibody specificity was confirmed by immunoblotting with rat lung lysates or human pulmonary smooth muscle cells. A single band at about 70 kDa was visible in the immunoblots.

Lung Immunohistochemistry and Immunofluorescence

Human IPAH and control lung samples were obtained from the Imperial College pulmonary hypertension biorepository (ethics reference numbers: 01-210 & 2001/6003) where samples are deposited following informed patient consent. Anonymised Kyrgyz high-altitude lung samples were obtained from post-mortem lung following approval of the local ethics committee (reference 02-23/880).

Lung sections were immunostained with rabbit anti-ZIP12 (1:1000), Ki67 (1:50; Thermo Scientific) and rabbit anti-CAIX (1:100) antibodies. For immunohistochemistry, horseradish peroxidase conjugated secondary anti-rabbit antibody (1:200) was used. Double immunofluorescence with anti-αSMA (1:100) was performed using fluorescence secondary antibodies, anti-mouse Alexa 488 and anti-rabbit Alexa 568 (1:2000, Invitrogen). Images (green for ZIP12 and red for αSMA) were detected under Leica confocal microscope (TCS SP2 AOBS).

Human pulmonary artery smooth muscle cell culture

Human pulmonary artery smooth muscle cells (HPASMCs) from PromoCell and Lonza were grown in Human Smooth Muscle Cell Growth Medium 2 (PromoCell). The cells were cultured under normal oxygen tension (20% O_2, 5% CO_2) or exposed to hypoxia (2% O_2, 5% CO_2, 92% N_2) for 48-72hr. A Bromodeoxyuridine (BrdU) cell proliferation assay (Millipore) was used to assess cell proliferation following manufacturer's conditions.

ZIP12 siRNA transfection

Cells were transfected overnight with 50pmol siRNA against ZIP12 (s8397, Ambion), or negative siRNA (4390844, Ambion) as a control, using Lipofectamine RNAiMAX (Invitrogen Life Technologies) according to manufacturer's conditions.

Quantification of actin fibre formation

Cells were cultured on plastic coverslips (Nunc), transfected with scramble or ZIP12 siRNA and exposed to hypoxia as described previously. After 48h exposure, cells were fixed with 4% formaldehyde solution in phosphate buffered saline (PBS) for 10 minutes at room temperature. Cells were then incubated with Alexa 568-conjugated phalloidin (1/200; Invitrogen) for F-actin detection under confocal microscopy. Sequential XYZ-sections (approximately 12 section of 1μm^2 / view) were obtained and 3D images were reconstructed. Quantification of actin stress fibres was determined by volume rendering in Image-J. Actin volume per cell was expressed as fold increase from normoxic control (value set at 1).

Quantification of zinc concentration by FRET measurement

Cells on coverslips were washed twice in Krebs-HEPES-bicarbonate (KHB) buffer (140mM NaCl, 3.6mM KCl, 0.5mM NaH_2PO_4, 0.2mM $MgSO_4$, 1.5mM $CaCl_2$, 10mM Hepes, 25mM $NaHCO_3$), which was warmed, bubbled with 95% O_2: 5% CO_2, set to pH 7.4, and contained

3mM glucose. Imaging of zinc using eCALWY sensors was carried out as optimized before[10,27]. Briefly, cells were maintained at 37°C throughout with a heating stage (MC60, LINKAM, Scientific Instruments), and KHB buffer was perfused (1.5 to 2ml/minute) with additions as stated in the Figures. Images were captured at 433 nm monochromatic excitation wavelength (Polychrome IV, Till photonics) using an Olympus IX-70 wide-field microscope with a 40x/1.35NA oil immersion objective and a zyla sCMOS camera (Andor Technology) controlled by Micromanager software[28]. Acquisition rate was 20 images/minute. Emitted light was split and filtered by a Dual-View beam splitter (Photometrics) equipped with a 505dcxn dichroic mirror and two emission filters (Chroma Technology - D470/24 for cerulean and D535/30 for citrine).

Image analysis was performed with ImageJ software[29] using a home-made macro and the fluorescence emission ratios were derived after subtracting background. Steady-state fluorescence intensity ratio citrine/cerulean (R) was measured, then maximum and minimum ratios were determined to calculate free Zn^{2+} concentration using the following formula: $[Zn^{2+}] = K_d \times (R_{max}-R)/(R-R_{min})$. The maximum ratio ($R_{max}$) was obtained upon intracellular zinc chelation with 50 μM TPEN and the minimum ratio (R_{min}) was obtain upon zinc saturation with 100 μM $ZnCl_2$ in the presence of the Zn^{2+} ionophore, pyrithione (5 μM)[10].

HIF-motif analysis and cloning

HOMER[9] was used to scan for HIF-1α and HIF-2α recognition motifs in the region 2kb up-stream and 1.5 kb down-stream of the ZIP12 transcription start site. Results with a HOMER score < 6.5 were discarded. A 5' region of ZIP12 gene containing these motif (HRE) (human (hg19) chr10:18,240,587-18,242,100) was cloned into the multicloning site of pGL4.10, which encodes the luciferase reporter gene *luc2*, by Gibson Assembly (NEB, E2611S). Three

nucleotide substitutions in the core of the predicted HIF1/2α binding site motif were created by site-mutagenic PCR to produce a disabling mutant (Figure 2 d).

Transfection and luciferase assay

HPASMCs were seeded in 24 well plates at 70-80% confluence. Cells were transfected with 300ng of each plasmid together with 2ng of Renilla plasmid using Lipofectamine® 2000 (Life Technologies), exposed to hypoxia and lysed according to the manufacturer's conditions. Luciferase activity was measured using Dual-Luciferase® Reporter Assay Chemistry (Promega) as previously described[30]. Experiments were repeated in two cells lines, n=6 per line.

Chromatin immunoprecipitation and PCR

Specific protein-DNA interactions were examined by chromatin immunoprecipitation (ChIP) followed by quantitive PCR (Chromatin immunoprecipitation Assay Kit, Millipore). Protein-DNA crosslinks were achieved by fixation with 1% formaldehyde for 10 minutes at room temperature. DNA-protein complexes from $2x10^6$ cells were sheared to lengths between 200 and 500 base-pairs by sonicator (Bioruptor). The precleared fragments were incubated with 10 μg of HIF-1α or HIF-2α specific antibody (Novus Biologicals), or without antibody (as a negative control) overnight, followed by immunoprecipitation by Protein A Agarose/Salmon Sperm DNA (50% Slurry). The crosslinks were reversed by heating at 65°C overnight, followed by Proteinase K digestion at 45°C for 2 hours. DNA was then recovered with QIAquick PCR purification kit (Qiagen) for quantitative PCR to prove affinity against ZIP12 promoter region (Figure 2d). Experiments were conducted in two separate cell lines (n=3 each) and gave the same result.

Quantitative PCR was performed as previously described in the methodology, using 1ul of DNA sample, and using the forward primer 5-TTTCCCAACCTGGGTCCTAT-3 and the

reverse primer 5-AGCAGCCAAAAAGCTTGCTA-3. Ct values were normalized compared to the values detected in the starting non-inmunoprecipitated DNA sample (input). Protein-DNA affinity was confirmed when normalized Ct values were above the basal levels measured in the negative control.

Quantitative real time RT-PCR

RNA was extracted from lungs using RNeasy Mini Kit (Qiagen). PCR was performed with an ABI 7500 Sequence Detection System (Applied Biosystems). Quantitative PCR was performed using a two-step protocol starting with cDNA synthesis using the ImProm-II™ Reverse Transcription System (Promega), followed by PCR using the Power SYBR Green PCR Master Mix (Applied Biosystems). A total of 100ng of cDNA per sample was used. All samples were amplified using biological triplicates with two technical replicates per sample. The 7500 Sequence Detection System software (Applied Biosystems) was used to obtain C_T values. Results were analysed using the comparative C_T method[31]. Samples were normalized to a reference gene, *Ubc* (for rat samples) or *Cyclophilin* (for human cell samples), to account for cDNA loading differences.

Western blot

Frozen rat tissues (lungs) and cell pellets were homogenized in RIPA buffer (50mM tris-HCl, pH 8.0, 150mM sodium chloride, 1.0% Igepal, 0.5% sodium deokycholate, 0.1% sodium dodecyl sulphate) (Sigma) supplemented with protease inhibitor (Roche). Western blotting was performed using Mini-PROTEAN® TGX™ Precast Gels (Bio-rad) following the manufacture's suggestions. Blots were incubated for 1h at room temperature with Anti-ZIP12 (1:10,000); Anti-HIF1α (1:1000, Novus Biological); or Anti-HIF2α (1:1000, Novus Biological). Proteins were detected by Clarity western ECL substrate (Bio-rad). Optical

densities of individual bands were measured using ImageJ software and protein expressions were standardised with Vinculin.

Statistical analysis

Data are presented as mean ± the standard error of the mean (SEM). Data were tested for normality using the Kolmogorov-Smirnov. All data were confirmed normally distributed with similar variance between comparator groups. Data were analysed using one-way ANOVA followed by Bonferroni post-test adjustment for multiple comparisons or unpaired t-test. Graphpad Prism was used for all statistical analysis.

Other Bioinformatics analyses

The Ensembl database[32] was mined with the BioMart tool[33] to identify all transcribed elements in the CI region. Search was limited to chromosome 17 between positions 85,072,475-93,347,758. PolyPhen analysis was used to predict the possible impact of described SNP on amino acid substitution on the structure and function of a human protein[34].

References

24 Truett, G. E. *et al.* Preparation of PCR-quality mouse genomic DNA with hot sodium hydroxide and tris (HotSHOT). *BioTechniques* **29**, 52, 54 (2000).

25 Aplin, A. C. & Nicosia, R. F. The rat aortic ring model of angiogenesis. *Methods in molecular biology* **1214**, 255-264, doi:10.1007/978-1-4939-1462-3_16 (2015).

26 Edwards, R. J. Targeting antipeptide antibodies toward cytochrome P450 enzymes. *Methods in molecular biology* **320**, 173-182, doi:10.1385/1-59259-998-2:173 (2006).

27 Bellomo, E. A. *et al.* Glucose regulates free cytosolic Zn(2)(+) concentration, Slc39 (ZiP), and metallothionein gene expression in primary pancreatic islet beta-cells. *The Journal of biological chemistry* **286**, 25778-25789, doi:10.1074/jbc.M111.246082 (2011).

28 Edelstein, A. *et al.* Computer control of microscopes using microManager. *Current protocols in molecular biology / edited by Frederick M. Ausubel et al.* **Chapter 14**, Unit14 20, doi:10.1002/0471142727.mb1420s92 (2010).

29 Schneider, C. A. *et al.* NIH Image to ImageJ: 25 years of image analysis. *Nat Methods* **9**, 671-675 (2012).

30 Pasquali, L. *et al.* Pancreatic islet enhancer clusters enriched in type 2 diabetes risk-associated variants. *Nature genetics* **46**, 136-143, doi:10.1038/ng.2870 (2014).

31 Schmittgen, T. D. & Livak, K. J. Analyzing real-time PCR data by the comparative C(T) method. *Nature protocols* **3**, 1101-1108 (2008).

32 Flicek, P. *et al.* Ensembl's 10th year. *Nucleic acids research* **38**, D557-562, doi:10.1093/nar/gkp972 (2010).

33 Haider, S. *et al.* BioMart Central Portal--unified access to biological data. *Nucleic acids research* **37**, W23-27, doi:10.1093/nar/gkp265 (2009).

34 Adzhubei, I. A. *et al.* A method and server for predicting damaging missense mutations. *Nat Methods* **7**, 248-249, doi:10.1038/nmeth0410-248 (2010).

Figure 1.

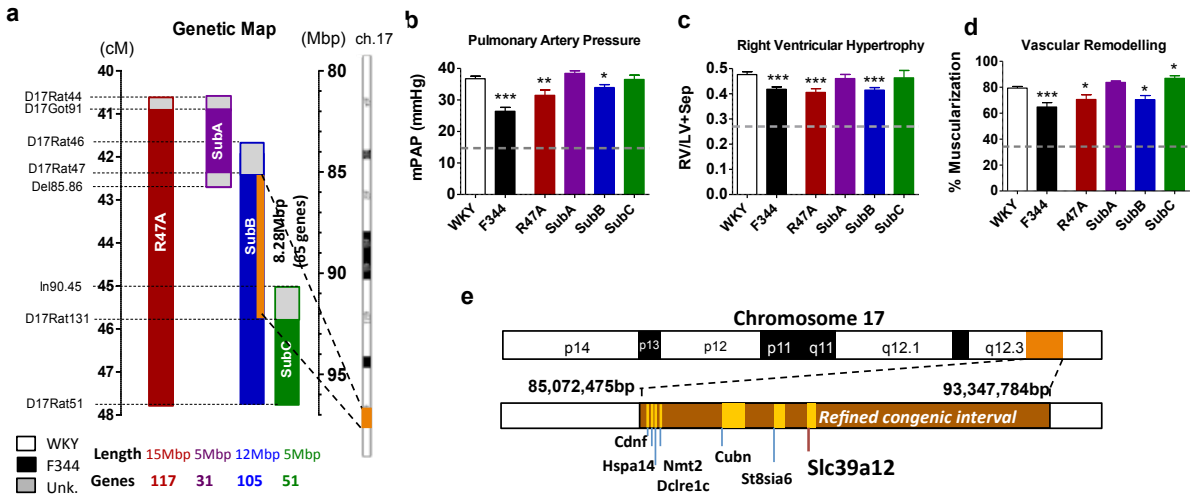

Figure 2.

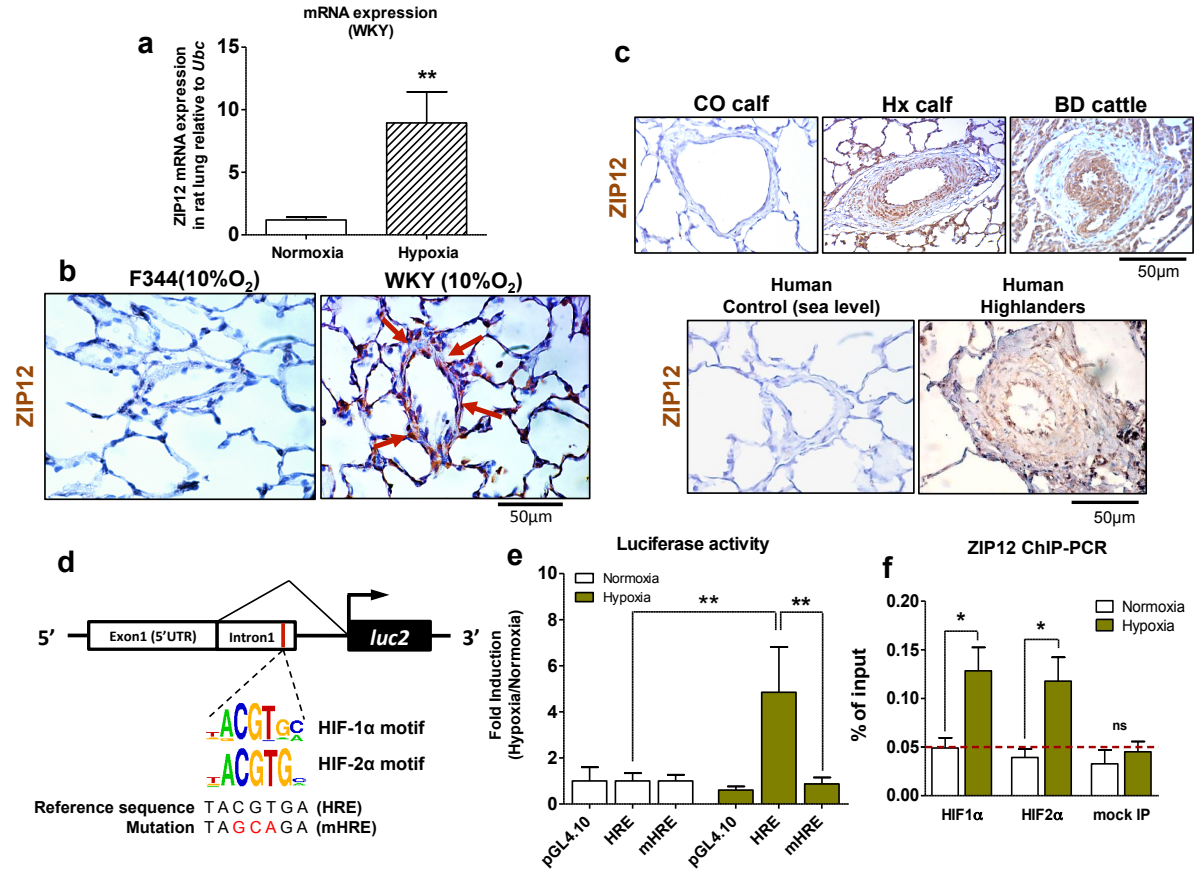

Figure 3.

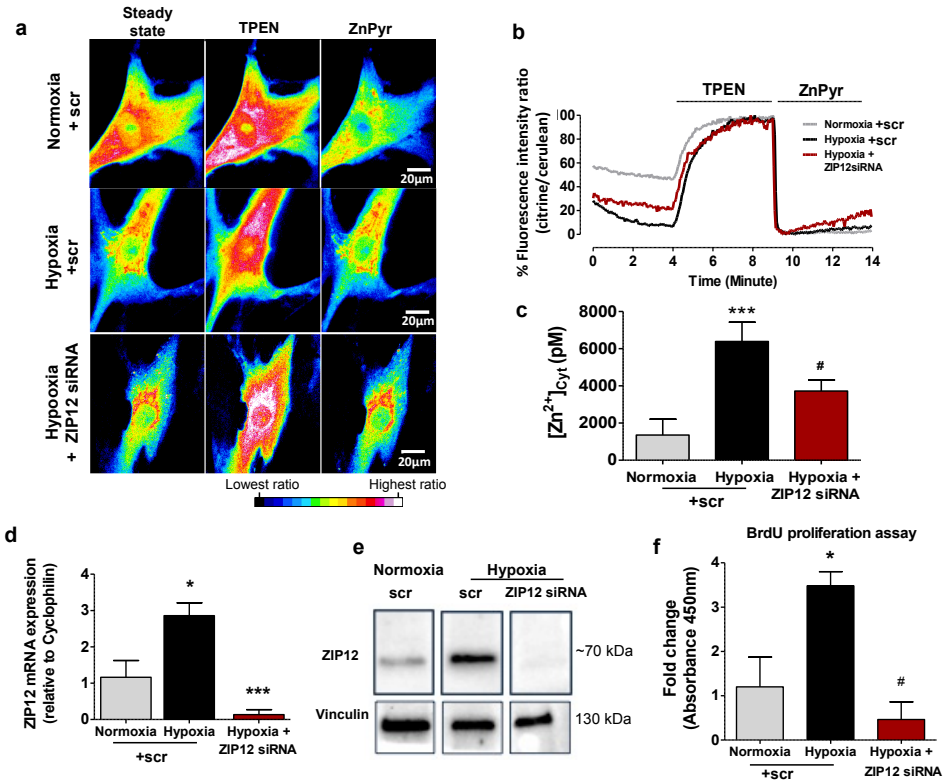

Figure 4.